Regional soil erosion assessment based on sample survey and geostatistics

Shuiqing Yin[1, 2], Zhengyuan Zhu[3], Li Wang[3], Baoyuan Liu[1, 2], Yun Xie[1, 2], Guannan Wang[4] and Yishan Li[1, 2]

[1]State Key Laboratory of Earth Surface Processes and Resource Ecology, Beijing Normal University, Beijing 100875, China

[2]School of Geography, Beijing Normal University, Beijing 100875, China

[3]Department of Statistics, Iowa State University, Ames 50010, USA

[4]Department of Mathematics, College of William & Mary, Williamsburg 23185, USA

Correspondence to: Baoyuan Liu (baoyuan@bnu.edu.cn)

Abstract. Soil erosion is one of the major environmental problems in China. From 2010-2012 in China, the fourth national census for soil erosion sampled 32,364 Primary Sampling Units (PSUs, small watersheds) with the areas of 0.2-3 km^2. Land use and soil erosion controlling factors including rainfall erosivity, soil erodibility, slope length, slope steepness, biological practice, engineering practice, and tillage practice for the PSUs were surveyed, and soil loss rate for each land use in the PSUs were estimated using an empirical model Chinese Soil Loss Equation (CSLE). Though the information collected from the sample units can be aggregated to estimate soil erosion conditions on a large scale, the problem of estimating soil erosion condition on a regional scale has not been well addressed. The aim of this study is to introduce a new model-based regional soil erosion assessment method combining sample survey and geostatistics. We compared five spatial interpolation models based on Bivariate Penalized Spline over Triangulation (BPST) method to generate a regional soil erosion assessment from the PSUs. Land use, rainfall erosivity, and soil erodibility at the resolution of 250×250 m pixels for the entire domain were used as the auxiliary information. Shaanxi province (3,116 PSUs) in China was used to conduct the comparison and assessment as it is one of the areas with the most serious erosion problem. The results showed three models with land use as the auxiliary information generated much lower mean squared errors (MSE) than the other two models without land use. The model assisted by the land use, rainfall erosivity factor (R), and soil erodibility factor (K) is the best one, which has MSE less than half that of the model smoothing soil loss in the PSUs directly. 56.5% of total land in Shaanxi province has annual soil loss

greater than 5 t ha^{-1} y^{-1}. High (20-40 t ha^{-1} y^{-1}), severe (40-80 t ha^{-1} y^{-1}) and extreme (>80 t ha^{-1} y^{-1}) erosion occupied 14.3% of the total land. The farmland, forest, shrub land and grassland in Shaanxi province had mean soil loss rates of 19.00, 3.50, 10.00, and 7.20 t ha^{-1} y^{-1}, respectively. Annual soil loss was about 198.7 Mt in Shaanxi province, with 67.8% of soil loss originated from the farmlands and grasslands in Yan'an and Yulin districts in the northern Loess Plateau region and Ankang and Hanzhong districts in the southern Qingba mountainous region. This methodology provides a more accurate regional soil erosion assessment and can help policy-makers to take effective measures to mediate soil erosion risks.

1 Introduction

With a growing population and a more vulnerable climate system, land degradation is becoming one of the biggest threats to food security and sustainable agriculture in the world. Water and wind erosion are the two primary causes of land degradation (Blanco and Lal, 2010). To improve the management of soil erosion and aid policy-makers to take suitable remediation measures and mitigation strategies, the first step is to monitor and assess the related system to obtain timely and reliable information about soil erosion conditions under present climate and land use. The risks of soil erosion under different scenarios of climate change and land use are also very important (Kirkby et al., 2008).

Scale is a critical issue in soil erosion modeling and management (Renschler and Harbor, 2002). When the spatial scale is small, experimental runoff plots, soil erosion markers (e.g. Caesium 137) or river sediment concentration measurement devices (e.g. optical turbidity sensors) are useful tools. However, when the regional scale is considered, it is impractical to measure soil loss across the entire region. A number of approaches were used to assess the regional soil erosion in different countries and regions over the world, such as expert-based factorial scoring, plot-based, field-based and model-based assessments, etc.

Factorial scoring was used to assess soil erosion risk when erosion rates are not required, and one only need a spatial distribution of erosion (CORINE, 1992; Guo and Li, 2009; Le Bissonnais et al., 2001). The classification or scoring of erosion factors (e.g. land use, rainfall erosivity, soil erodibility and slope) into discrete classes and the criteria used to combine the classes are based on expert experience. The resulting map depicts classes ranging from very low to very high erosion or erosion risk. However, factorial scoring approach has limitations on subjectivity and qualitative characteristics (Morgan, 1995; Grimm et al., 2002). Plot-based approach extrapolated the measurements from runoff plots to the region (Gerdan et al., 2010; Guo et al., 2015). However, Gerdan et al. (2010) discussed that the direct extrapolation may lead to poor estimation of regional erosion rates if the scale issue is not carefully taken into consideration. Evan et al., (2015) recommended a field-based approach combining visual interpretations of aerial and terrestrial photos and direct field survey of farmers' fields in Britain. However, its efficiency, transparency and accuracy were questioned (Panagos et al., 2016a). The model-based approach can not only assess soil loss up to the present time, but also has the advantage of assessing future soil erosion risk under different scenarios of climate change, land use and conservation practices (Kirkby et al., 2008; Panagos et al., 2015). USLE (Wischmeier and Smith, 1965; Wischmeier and Smith, 1978) is an empirical model based on the regression analyses of more than 10,000 plot-years of soil loss data in the USA and is designed to estimate long-term annual erosion rates on agricultural fields. (R)USLE (Wischmeier and Smith, 1978; Renard et al., 1997; Foster, 2004) and other adapted versions (for example, Chinese Soil Loss Equation, CSLE, Liu et al., 2002), are the most widely used models in the regional scale soil erosion assessment due to relative simplicity and robustness (Singh et al., 1992; Van der Knijff et al., 2000; Lu et al., 2001; Grimm et al., 2003; Liu, 2013; Bosco et al., 2015; Panagos et al., 2015). A physically based and spatially distributed model, the Pan-European Soil Erosion Risk (PESERA) model (Kirkby et al., 2000), is recommended for use in a policy framework (DPSIR, driving-force-pressure-state-impact-response) in Europe (Gobin et al., 2004). However, the input data required by the PESERA model was not always available with sufficient accuracy, which limited its use at regional and continental scale (Borrelli et al., 2016). Bosco et al. (2015) used an Extended RUSLE (e-RUSLE) model in the recent water erosion assessment in Europe due to its low-data demand. Panagos et al. (2015) presented the application of RUSLE2015 to estimate soil loss in Europe by introducing updated and high-resolution datasets for deriving soil erosion factors.

The applications of USLE and its related models in the assessment of regional soil erosion can be generally grouped into three categories. The first category is the area sample survey approach. One representative is the National Resource Inventory (NRI) survey on U.S. non-Federal lands (Nusser and Goebel, 1997; Goebel, 1998; Breidt and Fuller, 1999). The NRI survey has been conducted at 5-year interval since 1977, and changed to the current annual supplemented panel survey design in 2000. The point level soil erosion estimate is produced based on the USLE before 2007, and RUSLE estimate is produced after 2007. The 2012 NRI is the current NRI data, which provides nationally consistent data on the status, condition, and trends of land, soil, water, and related resources on the Nation's non-Federal lands for the 30-year period 1982-2012. USDA-NRCS (2015) summarized the results from the 2012 NRI, which also include a description of the NRI methodology and use. A summary of NRI results on rangeland is presented in Herrick et al. (2010). See for example Brejda et al. (2001), Hernandez, et al. (2013) for some applications using NRI data. Since a rigorous probability based area sampling approach is used to select the sampling sites, the design based approach is robust and reliable when it is used to estimate the soil erosion at the national and state level. However, due to sample size limitations, estimates at the sub-state level are more uncertain.

The second category is based on the multiplication of seamless grids. Each factor in the (R)USLE model is a raster layer and soil loss was obtained by the multiplication of numerous factors, which was usually conducted under GIS environment (Lu et al. 2001; Bosco et al., 2015; Panagos et al., 2015; Ganasri and Ramesh, 2015; Rao et al., 2015; Bahrawi et al., 2016). Raster multiplication is a popular model-based approach due to its lower cost, simpler procedures and easier explanation of resulting map. If the resolution of input data for the entire region is enough to derive all the erosion factors, raster multiplication approach is the best choice. However, there are several concerns about raster multiplication approach: (1) The information for the support practices factor (P) in the USLE was not easy to collect given the common image resolution and was not included in some assessments (Lu et al., 2001; Rao et al., 2015), in which the resulting maps don't reflect the condition of soil loss but the risk of soil loss. Without the information of P factor, it is also impossible to assess the benefit from the soil and water conservation practices. (2) The accuracy of soil erosion estimation for each cell is of concern if the resolution of database used to derive the erosion factors is limited. For example, Thomas et al. (2015) showed that the range of LS factor values derived from four sources of DEM (20 m DEM generated from 1:50,000 topographic maps, 30 m DEM from ASTER, 90 m DEM from shuttle radar topography mapping mission (SRTM) and 250 m DEM from global multi-resolution terrain elevation data (GMTED)) were considerably different, which suggested the grid resolutions of factor layers are critical and are determined by the data resolution used to derive the factor. A European water erosion assessment which introduced high-resolution (100 m) input layers reported the result that the mean soil loss rate in the European Union's erosion-prone lands was 2.46 t ha^{-1} y^{-1} (Panagos et al., 2015). This work is scientifically controversial mainly due to questions on these three aspects: (1) Should the assessment be based on the model simulation or the field survey? (2) Are the basic principles of the (R)USLE disregarded? and (3) Are the estimated soil loss rates realistic (Evans and Boardman, 2016; Fiener and Auerswald, 2016; Panagos et al., 2016a, b)? Panagos et al. (2006a, 2016b) argued that field survey method proposed by Evans et al. (2015) is not suitable for the application at the European scale mainly due to work force and time requirements. They emphasized their work focused on the differences and similarities between regions and countries across the Europe and RUSLE model with the simple transparent structure can achieve their goal if harmonized datasets were inputted.

The third category is based on the sample survey and geostatistics. One example is the fourth census on soil erosion in China, which was conducted during 2010-2012 (Liu, 2013). Ministry of Water Resources of the People's Republic of China (MWR) has organized four nationwide soil erosion investigations. The first three (in mid-1980s, 1999 and 2000) were mainly based on field survey, visual interpretation by experts and factorial scoring method (Wang et al., 2016). The third investigation used 30 m resolution of Landsat TM images and 1:50000 topography map. Six soil erosion intensities were classified mainly based on the slope for the arable land and a combination of slope and vegetation coverage for the non-arable land. The limitations for the first three investigations include the limited resolution of satellite images and topography maps, limited soil erosion factors considered (rainfall erosivity factor, soil erodibility factor, and practice factor were not considered), incapability of generating the soil erosion rate, and incapability of assessing the benefit from the soil and water conservation practices. The fourth census was based on a stratified unequal probability systematic sampling method (Liu et al., 2013). In total, 32,364 Primary Sampling Units (PSUs) were identified nationwide to collect factors for water erosion prediction (Liu, 2013). CSLE was used to estimate the soil loss for the PSUs. A spatial interpolation model was used to estimate the soil loss for the non-sampled sites.

Remote sensing technique has unparalleled advantage and potential in the work of regional scale soil erosion assessment (Veirling, 2006; Le Roux et al., 2007; Guo and Li, 2009; Mutekanga et al., 2010; El Haj El Tahir et al., 2010). The aforementioned assessment method based on the multiplication of erosion factors under GIS interface was largely dependent on the remote sensing dataset (Panagos et al., 2015b; Ganasri and Ramesh, 2015; Bahrawi et al., 2016), which also provide important information for the field survey work. For example, NRI relied exclusively on the high resolution remote sensing images taken from fixed wing airplanes to collect land cover information. However, many characteristics of soil erosion cannot be derived from remote sensing images. Other limitations include the accuracy of remote sensing data, the resolution of remote sensing images, financial constraints and so on, which result in some important factors influencing soil erosion being not available for the entire domain. It is important to note is that the validation is necessary and required to evaluate the performance of a specific regional soil erosion assessment method, although the validation process is difficult to implement in the regional scale assessment and is not well addressed in the existing literature (Gobin et al., 2004; Vrieling, 2006; Le Roux et al., 2007; Kirkby, et al., 2008).

There is an important issue arising in the regional soil erosion assessment based on survey sample, which is how to infer the soil erosion conditions including the extent, spatial distribution and intensity for the entire domain from the information of PSUs. NRI used primarily a design based approach to estimate domain level statistics.

While robust and reliable for large domains which contain enough sample sites, such method cannot be used to compute the estimate for the small domain. In the fourth census of soil erosion in China, a simple spatial model was used to smooth the proportion of soil erosion directly. Land use is one of the critical pieces of information in the soil erosion assessment (Ganasri and Ramesh, 2015) which is available for the entire domain. The erosion factors rainfall erosivity and soil erodibility are also available for the entire domain. The other factors including the slope length, slope degree, biological, engineering and tillage practice factors are either impossible or very difficult to obtain for the entire region at this stage. We sampled small watersheds (PSUs) to collect detailed topography information and conducted field survey to collect soil and water conservation practice information. The purpose of this study is to introduce a new regional soil erosion assessment method combining sample survey and geostatistics and compare five semi-parametric spatial interpolation models based on bivariate penalized spline over triangulation (BPST) method to generate regional soil loss (A) assessment from the PSUs. The five models are: smoothing A directly (Model I), estimating A assisted by R and K factors (Model II), estimating A assisted by land use (Model III), estimating A assisted by R and land use (Model IV) and estimating A assisted by R, K and land use (V). There are 3116 PSUs in the Shaanxi province and its surrounding areas which were used as an example to conduct the comparison and demonstrate assessment procedures (Fig. 1). For many regions in the world, data used to derive erosion factor such as conservation practice factor is often not available for all area, or the resolution is not adequate for the assessment. Therefore, the assessment method combining sample survey and geostatistics proposed in this study is valuable.

2 Data and Methods

2.1 Sample and field survey

The design of the fourth census on soil erosion in China is based on a map with Gauss–Krüger projection, where the whole China was divided into 22 zones with each zone occupying three longitude degrees width (From central meridian towards west and east 1.5 degrees each). Within each zone, beginning from the central meridian and the equator, we generated grids with a size of 40 km × 40 km (Fig. 2), which are the units at the first level (County level). The second level is Township level with a size of 10 km × 10 km. The third level is the control area, with a size of 5 km × 5 km. The fourth level is the 1 km × 1 km grid located in the middle of the control area. The 1 km × 1 km grid is the PSU in the plain area, whereas in the mountainous area, a small watershed with area between 0.2-3 km^2 which also intersects with the fourth level 1 km × 1 km grid is randomly picked as the PSU. The area for the mountainous PSU is restricted to be between 0.2-3 km^2, which is large enough for the enumerator and not too large to be feasible to conduct field work. There is a PSU within every 25 km^2, which suggests the designed sample density is about 4%. In practice, due to the limitation of financial resources, the surveyed sample density is 1% for most mountainous areas. The density of sample units in our survey depends on the level of uncertainty and the budget of the survey. We sampled a density of 4% in four experimental counties in different regions over China and found a density of 1% was acceptable given the current financial condition. The density for the plain area is reduced to 0.25% due to the lower soil erosion risk (Li et al., 2012). The field survey work for each PSU mainly included: (1) recording the latitude and longitude information for the PSU using a GPS; (2) drawing boundaries of plots in a base map of the PSU; (3) collecting the information of land use and soil conservation measures for each plot; and (4) taking photos of the overview of PSUs, plots and soil and water conservation measures for future validation. A plot was defined as the continuous area with the same land use, the same soil and water conservation measures, and the same canopy density and vegetation fraction in the PSU (difference <=10%, Fig. 3). For each plot, land use type, land use area, biological measures, engineering measures and tillage measures were surveyed. In addition, vegetation fraction was surveyed if the land use is a forest, shrub land or grassland. Canopy density is also surveyed if the land use is a forest.

2.2 Database of PSUs in Shaanxi and its surrounding areas

A convex hull of the boundary of Shaanxi province was generated, with a buffer area of 30 km outside of the convex hull (Fig. 4). The raster of R factor, K factor and 1:100000 land use map with a resolution of 250×250 m pixels for the entire area were collected. PSUs located inside the entire area were used, which included 1775 PSUs in the Shaanxi province and 1341 PSUs from the provinces surrounding the Shaanxi province, including Gansu (430), Henan (112), Shanxi (345), Inner Mongolia (41), Hubei (151), Chongqing (55), Sichuan (156) and Ningxia (51). There were 3116 PSUs in total. We had the information of longitude and latitude, land use type, land use area and factor values of R, K, L, S, B, E and T for each plot of the PSU. The classification system of the land use for the entire area and that for the survey units were not synonymous with each other. They were grouped into eight land use types include (1) farmland, (2) forest, (3) shrub land, (4) grassland, (5) water body, (6) construction land, (7) bare land and (8) unused land such as sandy land, Gebi and uncovered rock to make them corresponding to each other.

2.3 Soil loss estimation for the plot, land use and PSU

Soil loss for a plot can be estimated using CSLE equation as follows:

$$A_{uk} = R_{uk} \cdot K_{uk} \cdot L_{uk} \cdot S_{uk} \cdot B_{uk} \cdot E_{uk} \cdot T_{uk}, \quad (1)$$

where A_{uk} is the soil loss for the kth plot with the land use u (t ha^{-1} y^{-1}), R_{uk} is the rainfall erosivity (MJ mm ha^{-1} h^{-1} y^{-1}), K_{uk} is the soil erodibilty (t ha h MJ^{-1} ha^{-1} mm^{-1}), L_{uk} is the slope length factor, S_{uk} is the slope steepness factor, B_{uk} is the biological practice factor, E_{uk} is the engineering practice factor, T_{uk} is the tillage practice factor. The definitions of A, R and K are similar to that of USLE. Biological (B), Engineering (E) and Tillage (T) factor is defined as the ratio of soil loss from the actual plot with biological, engineering or tillage practices to the unit plot. Biological practices are the measures to increase the vegetation coverage for reducing runoff and soil loss such as trees, shrubs and grass plantation and natural rehabilitation of vegetation. Engineering practices refer to the changes of topography by engineering construction on both arable and non-arable land using non-normal farming equipment (such as earth mover) for reducing runoff and soil loss such as terrace, check dam and so on. Tillage practices are the measures taken on the arable land during ploughing, harrowing and cultivation processes using normal farming operations for reducing runoff and soil loss such as crop rotation, strip cropping and so on (Liu et al., 2002).

Liu et al. (2013) introduced the data and methods for calculating each factor. Here we present a brief introduction. Land use map with a scale of 1:100000 is from China's Land Use/cover Datasets (CLUD), which were updated regularly at a five-year interval from the late 1980s through the year of 2010 with standard procedures based on Landsat TM/ETM images (Liu et al., 2014). Land use map used in this study was the version of 2010 (Fig. 5a). 2678 weather and hydrologic stations with erosive daily rainfall from 1981 through 2010 were collected and used to generate the R factor raster map over the entire China (Xie et al., 2016). And for the K factor, soil maps with scales of 1:500,000 to 1:200,000 (for different provinces) from the Second National Soil Survey in 1980s generated more than 0.18 million polygons of soil attributes over mainland China, which was the best available spatial resolution of soil information we could collect at present. The physicochemical data of 16,493 soil samples (belong to 7764 soil series, 3366 soil families, 1597 soil subgroups and 670 soil groups according to Chinese Soil Taxonomy) from the maps and the latest soil physicochemical data of 1065 samples through the ways of field sampling, data sharing and consulting literatures were collected to generate the K factor for the entire country (Liang et al., 2013; Liu et al., 2013). We assumed the result of the soil survey could be used to estimate the K factor in our soil erosion survey. R factor raster map for the study area was clipped from the map of the country as well as the K factor raster map (Fig. 5b, c). Previous research showed topography factors should be derived from high resolution topography information (such as 1:10000 or larger scale topography contour map). Topography factors based on smaller scale of topography map (such as 1:50000 or 1:100000) in the mountainous and hilly area have large uncertainties. Topography contour maps with a scale of 1:10000 for the entire region were not available at present. Fig. 5d was based on SRTM 90m DEM dataset and it was used to demonstrate the variation in the topography, which was not used in the interpolation process due to its limited resolution. Topography contour map with a scale of 1:10000 for PSUs were collected to derive the slope lengths and slope degrees and to calculate the slope length factors and slope steepness factors (Fu et al., 2013). The land use map was used to determine the boundary of forest, shrub, and grass land. For these three land use types, MODIS NDVI and HJ-1 NDVI were combined to derive vegetation coverage. For the shrub and grass land, an assignment table was used to assign a value of the half-month B factor based on their vegetation coverage; For the forest land, the vegetation coverage derived from the aforementioned remote sensing data was used as the canopy density, which was combined with the vegetation fraction under the trees collected during the field survey to estimate the half-month B factor. The B factor for the whole year was weight-averaged by a weight of rainfall erosivity ratio for this half-month. Both C factor in Panagos et al. (2015) and B factor in this study for forest, shrub land and grassland were estimated based on the vegetation density derived from satellite images. The difference is that C factor in Panagos et al. (2015) for arable land and non-arable land was estimated separately based on different methodologies, whereas in this study, B factor was used to reflect biological practices on the forest, shrub land or grassland for reducing runoff and soil loss and T factor was used to reflect tillage practices on the farmland for reducing runoff and soil loss. For the farmland, biological factor equals 1 and for the other land uses, tillage factor equals 1. The engineering practice factor and tillage practice factor were assigned values based on the field survey and assignment tables for different engineering and tillage measures, which were obtained from published references (Guo et al., 2015).

In a PSU, there may be several plots within the same land use. Soil loss for the same land use was weight-averaged by the area of the plots with the same land use:

$$A_{ui} = \frac{\sum_{k=1}^{q}(\mathrm{A_{uik}S_{uik}})}{\sum_{k=1}^{q}\mathrm{S_{uik}}}, \quad (2)$$

where A_{ui} is the averaged soil loss for the land use u in the sample unit i; A_{uik} is the soil loss for the plot k with the land use u; S_{uik} is the area for the plot k with the land use u.

Soil loss for the entire PSU was weight-averaged by the area of the plots.

$$A_i = \frac{\sum_{p=1}^{N}(\mathrm{A_{ip}S_{ip}})}{\sum_{p=1}^{N}\mathrm{S_{ip}}}, \quad (3)$$

where A_i is the averaged soil loss for the sample unit i with N plots; A_{ip} is the soil loss for the plot p and S_{ip} is the area for the plot p.

2.4 Five spatial models based on BPST method

2.4.1 Five spatial models

Model I: Estimating A directly by spatial interpolation. Model I is a naive method which is used as a baseline for comparison. We treat unit i as a point, and use longitude and latitude information and A_i value of unit i to interpolate.

Model II: Estimating A with R and K as the auxiliary information. For any sampling unit i, let

$$Q_i = \frac{A_i}{R_i \cdot K_i}, \quad (4)$$

where R_i is the rainfall erosivity value for unit i , and K_i is the soil erodibility value for unit i. By smoothing Q_i 's over the domain using longitude and latitude information, we obtain the interpolation of Q_i 's over the entire domain. Then for the jth pixel on the domain, we estimate the soil loss A_j via

$$\hat{A}_j = \hat{Q}_j \cdot R_j \cdot K_j, \quad (5)$$

where $\hat{Q}_j$ is the estimator of Q_j .

Model III: Estimating A with the land use as the auxiliary information. For water body and unused area, the estimation of soil loss for the u^th land use and j^th pixel $\hat{A}_{uj}$ was set to be zero. For the rest land use types, A_{ui} for each land use was interpolated separately first and soil loss values for the entire domain $\hat{A}_{uj}$ are the combination of estimation for all land uses.

Model IV: Estimating A with R and land use as the auxiliary information. For any sampling unit i in land use u, define

$$T_{ui} = \frac{A_{ui}}{R_{ui}}, \qquad (6)$$

where R_{ui} is the rainfall erosivity value. For land use u, we smooth T_{ui}'s using the longitude and latitude information, and obtain the interpolation over the domain. For any j^th pixel in land use u, we estimate the soil loss A_{uj} by

$$\hat{A}_{uj} = \hat{T}_{uj} \cdot R_{uj}, \qquad (7)$$

where $\hat{T}_{uj}$ is the estimation of T_{uj} for the land use u and the pixel j.

Model V: Estimating A with R, K and land use as the auxiliary information. For land use u and sampling unit i, define

$$Q_{ui} = \frac{A_{ui}}{R_{ui} \cdot K_{ui}}, \qquad (8)$$

where K_{ui} is the soil erodibility value. For land use u, smoothing Q_{ui}'s over the domain, we obtain the estimator $\hat{Q}_{uj}$ of Q_{uj} for every pixel j. Then, for any j^th pixel in land use u, we can estimate the soil loss A_{uj} by

$$\hat{A}_{uj} = \hat{Q}_{uj} \cdot R_{uj} \cdot K_{uj}, \qquad (9)$$

2.4.2 Bivariate penalized spline over triangulation method

In spatial data analysis, there are mainly two approaches to make the prediction of a target variable. One approach (e.g., kriging) treats the value of a target variable at each location as a random variable and uses the covariance function between these random variables or a variogram to represent the correlation; another approach (e.g., spline or wavelet smoothing) uses a deterministic smooth surface function to describe the variations and connections among values at different locations. In this study, Bivariate Penalized Spline over Triangulation (BPST), which belongs to the second approach, was used to explore the relationship between location information in a two-dimensional (2-D) domain and the response variable. The BPST method we consider have several advantages. First, it provides good approximations of smooth functions over complicated domains. Second, the computational cost for spline evaluation and parameter estimation are manageable. Third, the BPST doesn't require the data to be evenly distributed or on regular-spaced grid. Since our data are a little sparse in some area, we employed the roughness penalties to regularize the spline fit; see the energy functional defined in equation (12). When the sampling is sparse in certain area, the direct BPST method may not be effective since the results may have high variability due to the small sample size. The penalized BPST is more suitable for this type of data because it can help to regularize the fit.

To be more specific, let $(x_i, y_i) \in \Omega$ be the latitude and longitude of unit i for $i = 1, 2, \dots, n$. Suppose we observe z_i at locations (x_i, y_i) and $\{(x_i, y_i, z_i)\}_{i=1}^{n}$ satisfy

$$z_i = f(x_i, y_i) + \varepsilon_i, i = 1,2, \dots, n, \qquad (10)$$

where ε_i's are random variables with mean zero, and $f(.)$ is some smooth but unknown function. To estimate f, we adopt the bivariate penalized splines on triangulations to handle irregular domains. In the following we discuss how to construct basis functions using bivariate splines on a triangulation of the domain Ω. Details of various facts about bivariate splines stated in this section can be found in Lai and Schumaker (2007). See also Guillas and Lai (2010) and Lai and Wang (2013) for statistical applications of bivariate splines on triangulations.

A triangulation of Ω is a collection of triangles $\Delta = \{\tau_1, \tau_2, \dots, \tau_N\}$ whose union covers Ω. In addition, if a pair of triangles in Δ intersects, then their intersection is either a common vertex or a common edge. For a given triangulation Δ, we can construct Bernstein basis polynomials of degree p separately on each triangle, and the collection of all such polynomials form a basis. In the following, let $S_r^p(\Delta)$ be a spline space of degree p and smoothness r over triangulation Δ. Bivariate B-splines on the triangulation are piecewise polynomials of degree p (polynomials on each triangle) that are smoothly connected across common edges, in which the connection of polynomials on two adjacent triangles is considered smooth if directional derivatives up to the r^{th} degree are continuous across the common edge.

To estimate f, we minimize the following penalized least square problem:

$$\min_{f \in S_r^p(\Delta)} \left(z_i - f(x_i, y_i)\right)^2 + \lambda \mathrm{PEN}(f), \qquad (11)$$

Where λ is the roughness penalty parameter, and PEN(f) is the penalty given below:

$$\mathrm{PEN(f)} = \int_{\tau\in\Delta} \left(\frac{\partial^2 f(x,y)}{\partial x^2}\right)^2 + \left(\frac{\partial^2 f(x,y)}{\partial x\,\partial y}\right)^2 + \left(\frac{\partial^2 f(x,y)}{\partial y^2}\right)^2 \mathrm{dxdy}, \quad (12)$$

For Models I-V defined in Section 2.4.1, we consider the above minimization to fit the model, and obtain the smoothed surface using the measurements of A (Models I and III) or Q (Models II and V) or T (Model IV) and their corresponding location information.

2.5 Assessment methods

To compare different models, we estimate the out-of-sample prediction errors of each method using the 10-fold cross validation. We randomly split all the observations over the entire domain (with the buffer zone) into ten roughly equal-sized parts. For each k = 1, 2, …., 10, we leave out part k, fit the model to the other nine parts (combined) inside the boundary with the buffer zone, and then obtain predictions for the left-out k^{th} part inside the boundary of Shaanxi Province. In the Model I and Model II, $MSE_{overall}$ is calculated as follows:

$$\mathrm{MSE_{overall}} = \frac{\sum_{k=1}^{10} \mathrm{SSE_k}}{n}, \quad (13)$$

In Models III, IV and V, we consider land use as one covariate. Therefore, the overall mean squared prediction error ($MSE_{overall}$) is calculated by the average of the sum of the product of individual MSE and the corresponding sample size. The overall $MSE_{overall}$ was calculated as follows: we first calculated the MSE of land each use u, u = 1, 2, ⋯, 8, similar as for Model I and Model II,

$$\mathrm{MSE_u} = \frac{\sum_{k=1}^{10} \mathrm{SSE_k}}{n}, \quad (14)$$

Then, the overall MSE can be calculated using

$$\mathrm{MSE_{overall}} = \frac{\sum_{u=1}^{8} \mathrm{MSE_u} * \mathrm{C_u}}{\sum_{u=1}^{8} \mathrm{C_u}}. \quad (15)$$

where C_u is the sample size for the land use u.

Six soil erosion intensity levels were divided according to the soil loss rate, which were mild (less than 5 t $ha^{-1}y^{-1}$), slight (5-10 t $ha^{-1}y^{-1}$), moderate (10-20 t $ha^{-1}y^{-1}$), high (20-40 t $ha^{-1}y^{-1}$), severe (40-80 t $ha^{-1}y^{-1}$), and extreme (greater than 80 t $ha^{-1}y^{-1}$), respectively. Each pixel in the entire domain was classified as an intensity level according to A_j or A_{uj}. The proportion of intensity levels, soil loss rates for different land uses and the spatial distribution of soil erosion intensity levels were based on the soil erosion conditions of pixels located inside of the Shaanxi boundary.

3 Results

3.1 Estimation for five models

Table 1 summarized the MSEs of the soil loss estimation based on different methods. Model V assisted by the rainfall erosivity factor (R), soil erodibility factor (K) and land use generated the least overall MSE values and the best result. MSE for Model V was 43.4% of that for Model I, and MSE for Model III assisted by the land use was 50.3% of Model I, which suggested that the land use is the key auxiliary information for the spatial model, which contributed much more information than R and K factors did.

3.2 Soil erosion intensity levels

These five models can be divided into two groups in the proportion pattern of soil erosion intensity levels (Fig. 6). The first group is two models without the land use as the auxiliary information (Model I and II) and the second group is three models assisted with the land use (Model III, IV and V). The first group generated no severe and extreme erosion levels and had a higher proportion of slight and moderate erosion levels than the second group. The second group generated a higher proportion of mild, severe and extreme erosion levels than the first group. Most severe and extreme erosion mainly occurred in the farmland and bare land (Fig. 7). The first group mainly underestimated the erosion degrees for the farmland and bare land and overestimated those for the forest, grassland and construction land. The main reason is when the land use is ignored, the extreme erosion levels, mostly in farmland and bare land, were smoothed by the surrounding low erosion levels, mostly in forest, shrub land, grassland and construction land.

The result of Model V with BPST method showed that the highest percentage is the mild erosion (43.5%), followed by the slight (21.3%), moderate (20.9%) and high erosion (10.1%). The severe and extreme erosion were 3.9% and 0.3%, respectively (Fig. 6). When it came to land use (Fig. 7), the largest percentage for the farmland was the high erosion, which occupied 26.6% of the total farmland. The severe and extreme erosion for the farmland were 11.3% and 0.9% of the total farmland, respectively. Most forest land and grassland had mild erosion (75.4% and 42.5%, respectively). Each of mild, slight and moderate erosion degrees occupied about 30% of the total shrub land.

3.3 Soil loss rates for different land uses

Fig. 8 showed soil loss rates for different land use generated from five models. Similar to the estimation of soil erosion intensity levels, the first group mainly underestimated the soil loss rates for the farmland and bare land

and overestimated those for the forest, grassland and construction land. The standard deviations of the farmland and bare land for the second group were much higher than those for the first group, which suggested the variation of soil loss rates for farmland and bare land pixels for the second group were greater than for the first group. The soil loss rate for four main land uses (farmland, forest, shrub land and grassland) by Model V was reported in Table 2.

3.4 Spatial distribution of soil erosion intensity

All five models simulated generally similar spatial patterns of soil erosion intensity (Fig. 9 (a)-(e)). Three models assisted with the land use (Model III, IV and V) showed more reasonable details (Fig. 9). Fig. 9(e) showed that severe and extreme soil erosion mainly occurred in the farmlands in the southern Qingba mountainous area. Fig 9(f) demonstrated the difference between Model V and Model I, which suggested Model I overestimated the erosion intensity levels for most forests and grasslands, whereas it underestimated the intensity of farmlands. The estimation from Model V showed that annual soil loss from Shaanxi province was about 198.7 Mt, 49.8% of which came from farmlands and 35.0% from grasslands (Table 3). The soil loss rate in Yan’an and Yulin in the northern part was 15.3 and 11.9 t ha^{-1} y^{-1} and ranked the highest among ten prefecture cities. About half of the soil loss for the entire province was from these two districts (Table 3). Ankang and Hanzhong in the southern part also had a severe soil loss rate and contributed about one quarter of soil loss for the entire province.

4 Discussion

The spatial pattern of soil erosion in Shaanxi province in this study is similar to the result of the third national investigation. Since the expert factorial scoring method didn't generate the erosion rate for each land use, we compared the percentage of soil erosion area for ten prefecture cities in Shaanxi province between the third and the fourth investigations. Both investigations indicated Yan’an, Yulin and Tongchuan in the northern part and Ankang in the southern part had the most serious soil erosion. The difference is that Hanzhong was underestimated and Shangluo was overestimated in the third investigation, compared with the fourth investigation. Guo et al. (2015) analyzed 2823 plot-year runoff and soil loss data from runoff plots across five water erosion regions in China and compared the results with previous research across the world. The results showed that there were no significant differences for the soil loss rates of forest, shrub land and grassland worldwide, whereas the soil loss rates of farmland with conventional tillage in northwest and southwest China were much higher than those in most other countries. Shaanxi province is located in the Northwest region. Soil loss rates for the farmland, forest, shrub land and grassland based on the plot data for the NW region in Guo et al. (2015) were extracted and presented in Table 2 for comparison. Soil loss rate for the farmland based on the plot data varied greatly with the management and conservation practices and the result in this study was within the range (Table 2). The soil loss rate for the shrub land is similar with that reported in Guo et al. (2015). The soil loss rate for the forest in this study was 3.50 t ha^{-1} y^{-1} with a standard deviation of 2.78 t ha^{-1} y^{-1} , which is much higher than 0.10 t ha^{-1} y^{-1} reported in Guo et al. (2015, Table 2). Our analysis showed that it came from the estimation of PSUs and was not introduced by the spatial interpolation process. Possible reasons include: the different definitions of forest and grassland, concentrated storms with intense rainfall, the unique topography in Loess plateau and the sparse vegetation cover due to intensive human activities (Zheng and Wang, 2014). The minimum canopy density (crown cover) threshold for the forest across the world vary from 10-30% (Lambrechts et al., 2009) and a threshold of 10% was used in this study, which suggests on average a lower cover coverage and higher B factor. Annual average precipitation varies between 328-1280 mm in Shaanxi, with 64% concentrating in June through September. Most rainfall comes from heavy storms of short duration, which suggests the erosivity density (rainfall erosivity per unit rainfall amount) is high. Field survey result on the PSUs in this study showed that the slope degree is steeper and slope length is longer for the forest than the forest plots in Guo et al. (2015). The forest plots in Guo et al. (2015) were with an averaged slope degree of 25.9 °and slope length of 21.1 m, whereas 74.0% of forest lands were with a slope degree greater than 25 °and 97.2% of them with a slope length longer than 20 m. The runoff and sediment discharge information for two watersheds (Fig. 1, Table 4) showed that the soil loss rate for the forest in study area has large variability ranging from 1.3 to 19.0 t ha^{-1} y^{-1} (Wang and Fan, 2002). Our estimation is within the range. The soil loss rate for the grassland in this study was 7.20 t ha^{-1} y^{-1}, which was smaller than 11.57 t ha^{-1} y^{-1} reported in Guo et al. (2015). The reason may be due to the lower slope degree for the grassland in Shaanxi province. The mean value of the slope degree for grassland plots was 30.7 °in Guo et al. (2015), whereas 68.6% of the grass lands were with a slope degree smaller than 30 °from the survey in this study.

Remarkable spatial heterogeneity of soil erosion intensity was observed in the Shaanxi province. The Loess Plateau region is one of the most severe soil erosion regions in the world due to seasonally concentrated and high intensity rainfall, high erodibility of loess soil, highly dissected landscape, and long-term intensive human activities (Zheng and Wang, 2014). Most of the sediment load in the Yellow River is originated and transported from the Loess Plateau. Recently, the sediment load of the Yellow River declined to about 0.3 billion tons per year from 1.6 billion tons per year in the 1970s, which benefited from the soil and water conservation practices taken in the Loess Plateau region (He, 2016). However, more efforts on controlling human accelerated soil erosion in the farmlands and grasslands are still needed. Soil erosion in southern Qingba mountainous region is also very serious, which may be due to the intensive rainfall, farming in the steep slopes and deforestation (Xi et al., 1997). According to the survey in Shaanxi province, 11.1% of the farmlands with a slope degree ranging 15-25° and 6.3% of them greater than 25° were without any conservation practices. Mountainous areas with a slope steeper than 25° need to be sealed off for afforestation (grass) without the disturbance of the human and livestock. For those farmlands with a slope degree lower than 25°, terracing and tillage practices are suggested which can greatly reduce the soil loss rate (Guo et al., 2015, Table 2).

The survey result showed that there were 26.5% of grasslands with a slope degree of 15-25° and 57.6% of them steeper than 25° without any conservation practices. Enclosure and grazing prohibition are suggested on the grasslands with steep slope and low vegetation coverage.

Note that CSLE, as well as USLE-based models, simulate sheet and rill erosion, so erosion from gullies is not taken into consideration in this study. Erosion from gullies is also very serious in the Loess Plateau area and there were more than 140,000 gullies with length longer than 500 m in Shaanxi province (Liu, 2013).

5 Conclusions

The regional soil erosion assessment focused on the extent, intensity, and distribution of soil erosion on a regional scale and it provides valuable information to take proper conservation measures in erosion areas. Shaanxi province is one of the most severe soil erosion regions in China. A field survey in 3116 PSUs in the Shaanxi province and its surrounding areas were conducted, and the soil loss rates for each land use in the PSU were estimated from an empirical model (CSLE). Five spatial interpolation models based on BPST method were compared in generating regional soil erosion assessment from the PSUs. Following are our conclusions:

Land use is the key auxiliary information and R and K factors provide some useful information for the spatial geostatistical models in regional soil erosion assessment.

Our results show that 56.5% of total land had annual soil loss rate greater than 5 t ha^{-1} y^{-1}, and total annual soil loss amount is about 198.7 Mt in Shaanxi province. Most soil loss originated from the farmlands and grass lands in Yan'an and Yulin districts in the northern Loess Plateau region, and Ankang and Hanzhong districts in the southern Qingba mountainous region. Special attention should be given to the 0.11 million km^2 of lands with soil loss rate greater than 5 t ha^{-1} y^{-1}, especially 0.03 million km^2 of farmlands with severe erosion (greater than 20 t ha^{-1} y^{-1}).

A new model-based regional soil erosion assessment method was proposed, which is valuable when input data used to derive soil erosion factors is not available for the entire region, or the resolution is not adequate. When the resolution of input datasets was not adequate to derive reliable erosion factor layers and the budget is limited, our suggestion is sampling a certain amount of small watersheds as primary sampling units and put the limited money into these sampling units to ensure the accuracy of soil erosion estimation in these units. Limited money could be used to collect high resolution data such as satellite images and topography maps and conduct field survey to collect information such as conservation practices for these small watersheds. Then we can use the best available raster layers for land use, R, and K factor for the entire region, construct spatial model to exploit the spatial dependence among the other factors, and combine them to come up with better regional estimates. The information collected in the survey and the generated soil erosion degree map (such as Fig. 9e) can help policy-makers to take suitable erosion control measures in the severely affected areas. Moreover, climate and management scenarios could be developed based on the database collected in the survey process to help policy-makers in decision making for managing soil erosion risks.

Acknowledgments

This work was supported by the National Natural Science Foundation of China (No. 41301281), and the China Scholarship Council.

References

Bahrawi, J. A., Elhag, M., Aldhebiani, A. Y., Galal, H. K., Hegazy, A. K., and Alghailani, E.: Soil erosion estimation using remote sensing techniques in Wadi Yalamlam Basin, Saudi Arabia. Adv Mater Sci Eng, Article ID 9585962, 8 pages, http://dx.doi.org/10.1155/2016/9585962, 2016.

Blanco, H., and Lal, R.: Principles of Soil Conservation and Management. Springer, New York, 2010.

Borrelli, P., Paustian, K., Panagos, P., Jones, A., Schütt, B., and Lugato, E.: Effect of good agricultural and environmental conditions on erosion and soil organic carbon balance: A national case study. Land use policy, 50, 408–421, 2016.

Bosco, C., de Rigo, D., Dewitte, O., Poesen, J., and Panagos, P.: Modelling soil erosion at European scale towards harmonization, Nat Hazards Earth Syst Sci, 15, 225–245, 2015.

Breidt, F. J., and Fuller, W. A.: Design of supplemented panel surveys with application to the National Resources Inventory. J Agr Biol Envir St, 4, 391–403, 1999.

Brejda, J. J., Mausbach, M. J., Goebel, J. J., Allan, D. L., Dao, T. H., Karlen, D. L., Moorman, T. B., and Smith J. L.: Estimating surface soil organic carbon content at a regional scale using the National Resource Inventory. Soil Sci Soc Am J, 65(3), 842-849, 2001.

Cerdan, O., Govers, G., Le Bissonais, Y., Van Oost, K., Poesen, J., Saby, N., Gobin, A., Vacca, A., Quinton, J., Auerswald, K., Klik, A., Kwaad, F. J. P. M., Raclot, D., Ionita, I., Rejman, J., Rousseva, S., Muxart, T., Roxo, M. J., and Dostal, T.: Rates and spatial variations of soil erosion in Europe: a study based on erosion plot data. Geomorphology, 122, 167–177, 2002.

CORINE: Soil Erosion Risk and Important Land Resources in the Southern Regions of the European Community. European Commission, EUR 13233 EN, Luxembourg, 1992.

El Haj El Tahir, M., Kääb, A., and Xu, C. Y.: Identification and mapping of soil erosion areas in the Blue Nile, Eastern Sudan using multispectral ASTER and MODIS satellite data and the SRTM elevation model. Hydrol Earth Syst Sci, 14, 1167–1178, 2010.

Evans, R., and Boardman, J.: The new assessment of soil loss by water erosion in Europe. Panagos P. et al., 2015 Environ Sci Policy 54, 438–447—A response. Environ Sci Policy, 58, 11–15, 2016.

Evans, R., Collins, A. L., Foster, I. D. L., Rickson, R. J., Anthony, S. G., Brewer, T., Deeks, L., Newell-Price, J. P., Truckell, I. G., and Zhang, Y.: Extent, frequency and rate of water erosion of arable land in Britain—benefits and challenges for modelling. Soil Use Manage, 32(S1), 149–161, 2015.

Fiener, P., and Auerswald, K.: Comment on "The new assessment of soil loss by water erosion in Europe" by Panagos et al. (Environmental Science & Policy 54 (2015) 438–447). Environ Sci Policy, 57, 140–142, 2016.

Foster, G. R.: User's Reference Guide: Revised Universal Soil Loss Equation (RUSLE2). U.S. Department of Agriculture, Agricultural Research Service, Washington DC, 2004.

Fu, S. H., Wu, Z. P., Liu, B. Y., and Cao, L. X.: Comparison of the effects of the different methods for computing the slope length factor at a watershed scale. Int Soil Water Conserv Res, 1(2), 64–71, 2013.

Ganasri, B. P., and Ramesh, H.: Assessment of soil erosion by RUSLE model using remote sensing and GIS - A case study of Nethravathi Basin. Geoscience Frontiers, 7(6), 953–961, 2015.

Gobin, A., Jones, R., Kirkby, M. J., Campling, P., Govers, G., Kosmas, C., and Gentile, A. R.: Indicators for pan-European assessment and monitoring of soil erosion by water. Environ Sci Policy, 7, 25–38, 2004.

Goebel, J. J.: The National Resources Inventory and its role in U.S. agriculture. Agricultural Statistics 2000. International Statistical Institute, Voorburg, 1998.

Grimm, M., Jones, R., and Montanarella, L.: Soil erosion risk in Europe. European Commission, Joint Research Centre, EUR 19939 EN, Ispra, 2002.

Grimm, M., Jones, R., Rusco, E. and Montanarella, L.: Soil Erosion Risk in Italy: a revised USLE approach. European Commission, EUR 20677 EN, Luxembourg, 2003.

Guillas, S., and Lai, M. J.: Bivariate splines for spatial functional regression models. J Nonparametr Statist, 22, 477–497, 2010.

Guo, Q. K., Hao,Y. F., and Liu, B. Y.: Rates of soil erosion in China: A study based on runoff plot data. Catena, 24, 68–76, 2015.

Guo, Q. K., Liu, B. Y., Xie, Y., Liu, Y. N., and Yin, S. Q.: Estimation of USLE crop and management factor values for crop rotation systems in China. J Integr Agr, 14(9), 1877–1888, 2015.

Guo, S. Y., and Li, Z. G.: Development and achievements of soil and water conservation monitoring in China. Science of soil and water conservation, 7(5), 19–24, 2009 (in Chinese with English abstract).

He, C. S.: Quantifying drivers of the sediment load reduction in the Yellow River Basin. National Sci Rev, 00, 1–2, doi: 10.1093/nsr/nww014, 2016.

Hernandez, M., Nearing, M. A., Stone, J. J., Pierson, E. B., Wei, H., Spaeth, K. E., Heilman, P., Weltz, M. A., and Goodrich, D. C.: Application of a rangeland soil erosion model using National Resources Inventory data in southeastern Arizona. J Soil Water Conserv 68(6), 512–525, 2013.

Herrick, J. E., Lessard, V. C., Spaeth, K. E., Shaver, P. L., Dayton, R. S., Pyke, D. A., Jolley, L., and Goebel, J. J.: National ecosystem assessments supported by scientific and local knowledge. Front Ecol Environ, 8(8), 403–408, 2010.

Kirkby, M. J., Irvine, B. J., Jones, R. J. A., Govers, G., Boer, M., Cerdan, O., Daroussin, J., Gobin, A., Grimm, M., Le Bissonnais, Y., Kosmas, C., Mantel, S., Puigdefabregas, J., and van Lynden, G.: The PESERA coarse scale erosion model for Europe. I.–Model rationale and implementation. Eur J Soil Sci, 59, 1293–1306, 2008.

Kirkby, M. J., Le Bissonais, Y., Coulthard, T. J., Daroussin, J., and McMahon, M. D.: The development of land quality indicators for soil degradation by water erosion. Agric Ecosyst Environ, 81, 125–136, 2000.

Lai, M. J., and Schumaker, L. L.: Spline functions on triangulations. Cambridge University Press, Cambridge, 2007.

Lai, M. J., and Wang, L.: Bivariate penalized splines for regression. Statist Sinica, 23, 1399–1417, 2013.

Le Bissonnais, Y., Montier, C., Jamagne, M., Daroussin, J., and King, D.: Mapping erosion risk for cultivated soil in France. Catena, 46(2–3), 207–220, 2001.

Le Roux, J. J., Newby, T. S., and Sumner, P. D.: Monitoring soil erosion in South Africa at a regional scale: review and recommendations. S Afr J Sci, 207(103), 329–335, 2007.

Li, Z. G., Fu, S. H., and Liu, B. Y.: Sampling program of water erosion inventory in the first national water resource survey. Sci Soil Water Conserv, 10(1), 77–81, 2012 (in Chinese with English abstract).

Liang, Y., Liu, X. C., Cao, L. X., Zheng, F. L., Zhang, P. C., Shi, M. C., Cao, Q. Y., and Yuan, J. Q.: K value calculation of soil erodibility of China water erosion areas and its Macro-distribution. Soil Water Conserv in China, 10, 35–40, 2013 (in Chinese with English abstract).

Liu, B. Y., Zhang, K. L., and Xie, Y.: An empirical soil loss equation in: Proceedings–Process of soil erosion and its environment effect (Vol. II), 12th international soil conservation organization conference, Tsinghua University Press, Beijing, 21–25, 2002.

Liu, B. Y., Guo, S. Y., Li, Z. G., Xie, Y., Zhang, K. L., and Liu, X. C.: Sample survey on water erosion in China. Soil Water Conserv in China, 10, 26–34, 2013 (in Chinese with English abstract).

Liu, J. Y., Kuang, W. H., Zhang, Z. X., Xu, X. L., Qin, Y. W., Ning, J., Zhou, W. C., Zhang, S. W., Li, R. D., Yan, C. Z., Wu, S. X., Shi, X. Z., Jiang, N., Yu, D. S., Pan, X. Z., and Chi, W. F.: Spatiotemporal characteristics, patterns and causes of land use changes in China since the late 1980s. Acta Geographica

Sinica, 69(1): 3–14, 2014 (in Chinese with English abstract).

Liu, Z.: The national census for soil erosion and dynamic analysis in China. Int Soil Water Conserv Res, 1(2), 12–18, 2003.

Lu, H., Gallant, J., Prosser, I. P., Moran, C., and Priestley, G.: Prediction of sheet and rill erosion over the Australian continent, incorporating monthly soil loss distribution. CSIRO Land and Water Technical Report, Canberra, 2001.

Morgan, R. P. C.: Soil Erosion and Conservation, Second Edition. Longman, Essex, 1995.

Mutekanga, F. P., Visser, S. M., Stroosnijder, L.: A tool for rapid assessment of erosion risk to support decision-making and policy development at the Ngenge watershed in Uganda. Geoderma, 160, 165–174, 2010.

Nusser, S. M., and Goebel, J. J.: The National Resources Inventory: A long-term multi-resource monitoring programme. Environ Ecol Stat, 4(3), 181– 204, 1997.

Panagos, P., Borrelli, P., Poesen, J., Ballabio, C., Lugato, E., Meusburger, K., Montanarella, L., and Alewell, C.: The new assessment of soil loss by water erosion in Europe. Environ Sci Policy, 54, 438–447, 2015.

Panagos, P., Borrelli, P., Poesen, J., Meusburger, K., Ballabio, C., Lugato, E., Montanarella, L., and Alewell, C.: Reply to "The new assessment of soil loss by water erosion in Europe. Panagos P. et al., 2015 Environ. Sci. Policy 54, 438–447—A response" by Evans and Boardman [Environ. Sci. Policy 58, 11–15]. Environ Sci Policy, 59, 53–57, 2016a.

Panagos, P., Borrelli, P., Poesen, J., Meusburger, K., Ballabio, C., Lugato, E., Montanarella, L., and Alewell, C.: Reply to the comment on "The new assessment of soil loss by water erosion in Europe" by Fiener & Auerswald. Environ Sci Policy, 57, 143–150, 2016b.

Rao, E. M., Xiao, Y., Ouyang, Z. Y., and Yu, X. X.: National assessment of soil erosion and its spatial patterns in China. Ecosystem Health and Sustainability, 1(4), 13, doi: 10.1890/EHS14-0011.1, 2015.

Renard, K. G., Foster, G. R.,Weesies, G. A., McCool, D. K., and Yoder, D. C.: Predicting soil erosion by water. U.S. Department of Agriculture, Agricultural Research Service, Agriculture Handbook 703, Washington DC, 1997.

Renschler, C. S., and Harbor, J.: Soil erosion assessment tools from point to regional scales—the role of geomorphologists in land management research and implementation. Geomorphology, 47, 189–209, 2002.

Singh, G., Babu, R., Narain, P., Bhushan, L. S., and Abrol, I. P.: Soil erosion rates in India. J Soil Water Cons, 47 (1), 97–99, 1992.

Thomas, J., Prasannakumar, V., and Vineetha, P.: Suitability of spaceborne digital elevation models of different scales in topographic analysis: an example from Kerala, India. Environ Earth Sci, 73, 1245-1263, 2015.

USDA: Summary report: 2012 National Resources Inventory. National Resources Conservation Service, Washington DC, and Center for Survey Statistics and Methodology, Iowa State University, Ames, Iowa, 2015.

Van der Knijff, J. M., Jones, R. J. A., and Montanarella, L.: Soil erosion risk assessment in Europe. European Commission, EUR 19044 EN, Luxembourg, 2000.

Vrieling, A.: Satellite remote sensing for water erosion assessment: A review. Catena, 65, 2–18, 2006.

Wang, G., and Fan, Z.: Study of Changes in Runoff and Sediment Load in the Yellow River (II). Yellow River

Water Conservancy Press, Zhengzhou, China, 2002 (in Chinese).

Wang, X., Zhao, X. L., Zhang, Z. X., Li, L., Zuo, L. J., Wen, Q. K., Liu, F., Xu, J. Y., Hu, S. G., and Liu, B.: Assessment of soil erosion change and its relationships with land use/cover change in China from the end of the 1980s to 2010. Catena, 137, 256-268, 2016.

Wischmeier, W. H., and Smith, D. D.: Predicting Rainfall Erosion Losses: A Guide to Conservation Planning. U.S. Department of Agriculture, Agricultural Research Service, Agriculture Handbook 537, Washington DC, 1978.

Wischmeier, W. H., and Smith, D. D.: Predicting rainfall-erosion losses from cropland east of the Rocky Mountains. U. S. Department of Agriculture, Agricultural Research Service, Agriculture Handbook 282, Washington DC, 1965.

Xi, Z. D., Sun, H., and Li, X. L.: Characteristics of soil erosion and its space-time distributive pattern in southern mountains of Shaanxi province, Bull Soil Water Conserv, 17(2), 1–6, 1997 (in Chinese with English abstract).

Xie, Y., Yin, S. Q., Liu, B. Y., Nearing M., and Zhao, Y.: Models for estimating daily rainfall erosivity in China. J Hydrol, 535, 547–558, 2016.

Zheng, F. L., and Wang, B.: Soil Erosion in the Loess Plateau Region of China. Tsunekawa A. et al. (eds.), Restoration and Development of the Degraded Loess Plateau, China, Ecological Research Monographs. Springer, Japan, doi.10.1007/978-4-431-54481-4_6, 2014.

Tables

Table 1. Mean squared errors of soil loss (A) using bivariate penalized spline over triangulation (BPST)

Model	Land use and sample size						Overall
	Farmland	Forest	Shrub land	Grassland	Construction land	Bare land	
	1134	1288	573	683	401	32	4111
I	—	—	—	—	—	—	352.5
II	—	—	—	—	—	—	345.5
III	399.7	25.3	45.5	20.0	165.7	4264.6	177.2
IV	404.3	25.3	45.4	19.5	164.5	3691.2	173.8
V	365.4	24.3	38.0	16.3	162.5	3555.1	152.9

Table 2. Soil loss rates (t ha^{-1}y^{-1}) for the farmland, forest, shrub land and grassland by Model V in this study and in Northwest region of China from Guo et al. (2015).

	Land use	Mean	Standard deviation
This study	Farmland	19.00	17.94
	Forest	3.50	2.78
	Shrub land	10.00	7.51
	Grassland	7.20	5.23
Guo et al. (2015)	Farmland (Conventional)	49.38	57.61
	Farmland (Ridge tillage)	19.27	13.35
	Farmland (Terracing)	0.12	0.28
	Forest	0.10	0.12
	Shrub land	8.06	7.47
	Grassland	11.57	12.72

Table 3. Annual soil loss amount, rate and main sources by Model V for ten prefecture cities in Shaanxi province.

Prefecture city	Area (10^4 ha)	Amount (10^6 t y^{-1})	Rate (t ha^{-1} y^{-1})	Source (%)			
				Farmland	Forest	Shrub land	Grass land
Xi'an	100.4	6.3	6.3	52.9	11.6	7.9	20.6
Ankang	230.0	26.6	11.6	42.8	10.7	2.8	42.7
Baoji	178.5	13.2	7.4	39.3	15.1	7.5	37.9
Hanzhong	266.7	21.8	8.2	42.5	12.3	3.6	40.2
Shangluo	193.0	8.5	4.4	68.0	13.1	5.9	12.9
Tongchuan	38.6	3.7	9.6	37.9	7.8	23.6	28.5
Weinan	129.5	6.4	5.0	54.4	3.9	9.5	26.7
Xianyang	101.0	5.2	5.2	44.4	8.2	8.9	35.3
Yan'an	364.9	55.9	15.3	54.5	3.1	12.1	30.0
Yulin	427.7	50.9	11.9	51.4	2.6	3.7	40.4
Overall	2030.4	198.7	9.8	49.8	6.8	7.1	35.0

Table 4 Soil erosion rate for the forest and sediment discharge for two watersheds

	Area (10^4 ha)	Runoff (10^9 m^3 y^{-1})	Sediment discharge (10^6 t y^{-1})	Soil loss rate (t ha^{-1} y^{-1})	Percent of forest (%)	Soil loss rate for forest (t ha^{-1} y^{-1})
Jinghe[a]	454.2	1.837	246.7	54.3	6.5	19.0
Luohe[b]	284.3	0.906	82.6	29.1	38.4	1.3~2.1

[a.] Based on the observation at Zhangjiashan hydrological station from 1950 through 1989.

[b.] Based on the observation of at Zhuanghe hydrological station from 1959 through 1989.

Figures

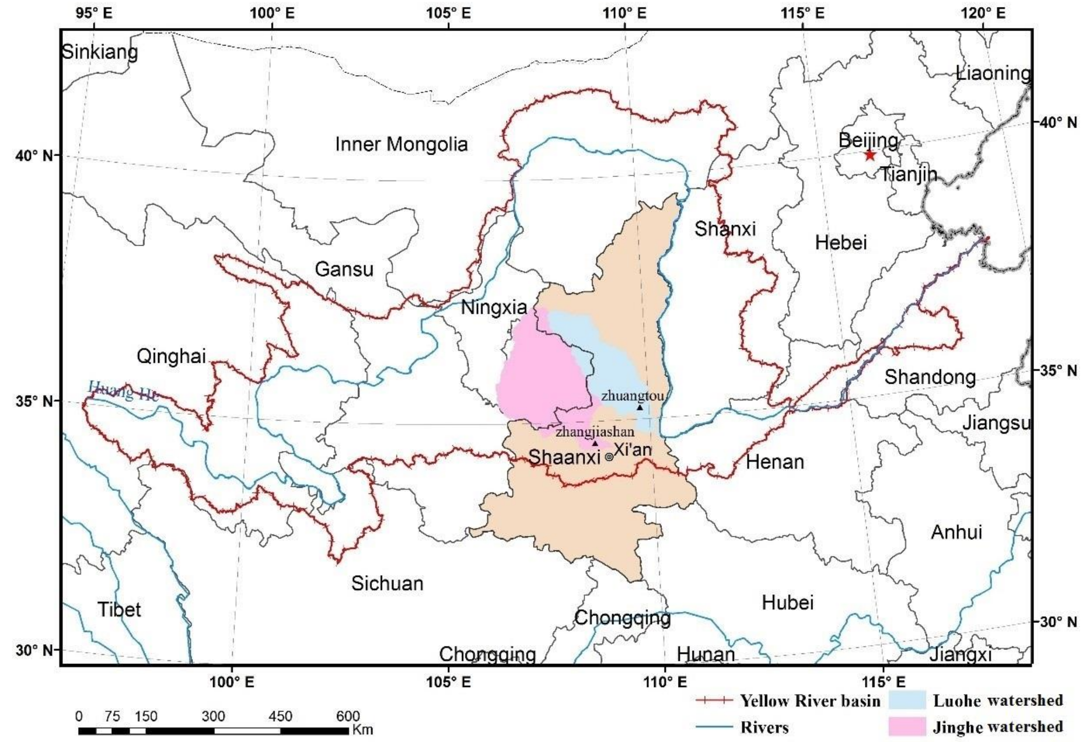

Figure 1: Location of Shaanxi province. Luohe and Jinghe watersheds were referred in the Table 4 and discussion part.

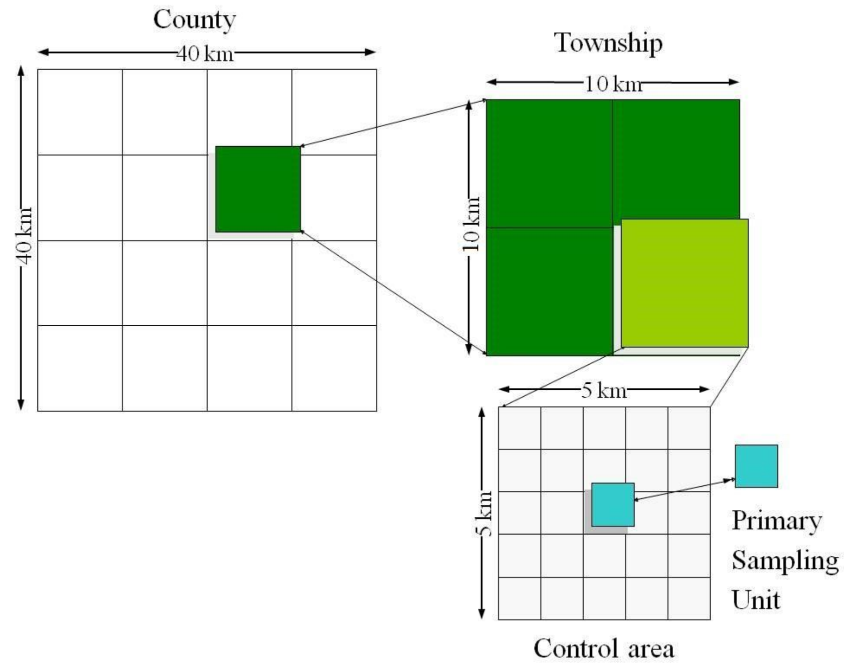

Figure 2: Schematic of sampling strategy for the fourth census on soil erosion in China

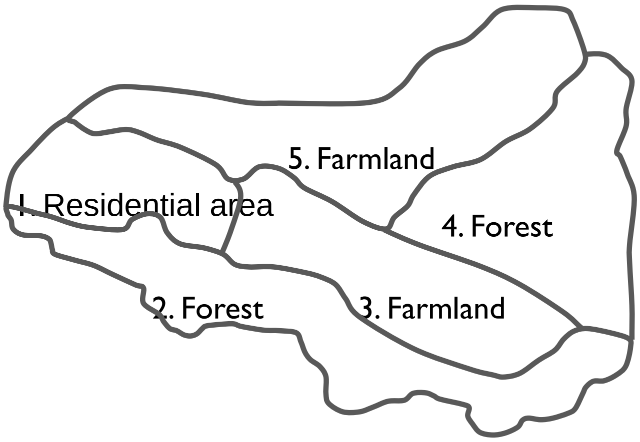

Figure 3: An example of a PSU with five plots and three categories of land uses (Farmland, Forest and Residential area).

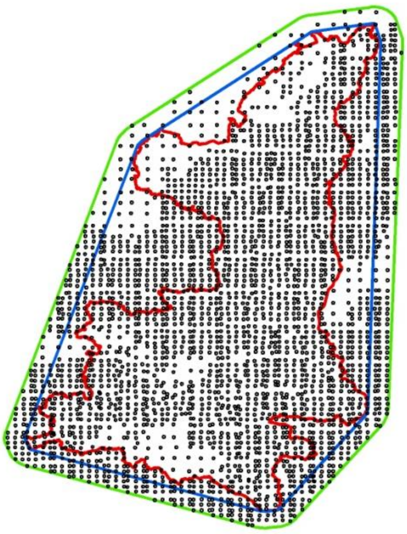

Figure 4: Distribution of PSUs (solid dots) used in this study. The red line is the boundary of the Shaanxi province, blue line is the convex hull of the boundary and green line is the 30 km buffer of the convex hull.

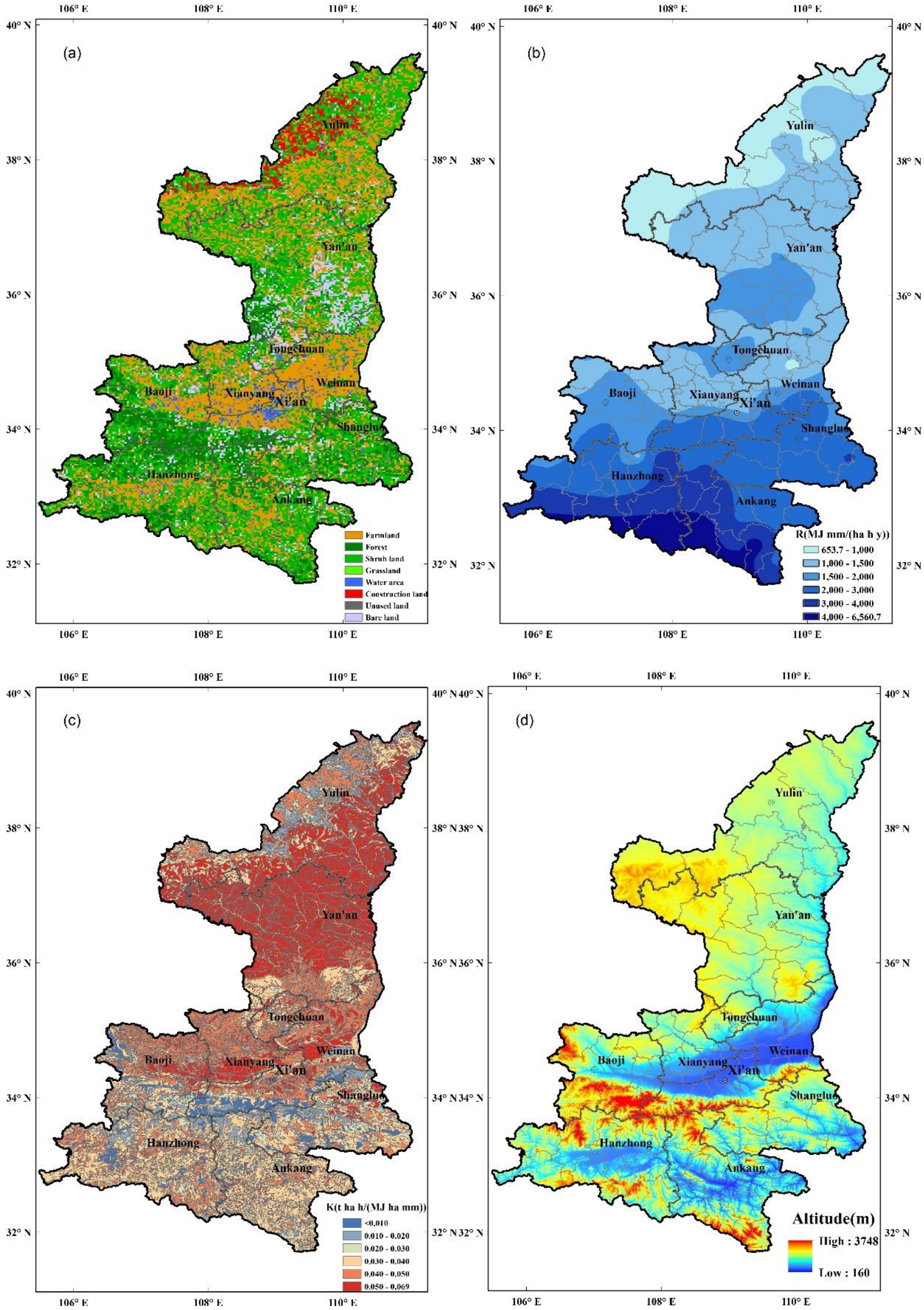

Figure 5 Spatial distributions of land use (a), rainfall erosivity (b), soil erodibility (c) and topography (d) for Shaanxi province.

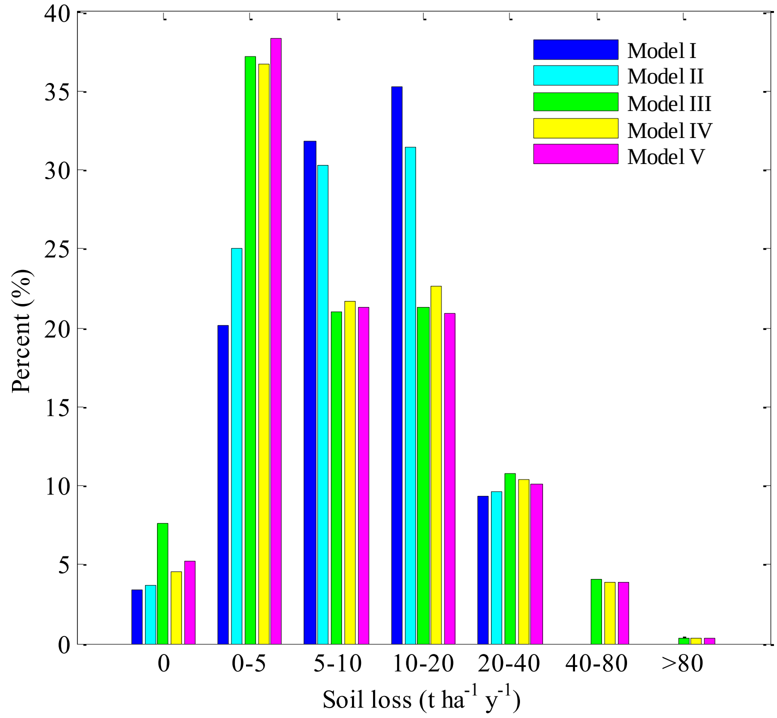

Figure 6: Proportion of soil erosion intensity levels for five models.

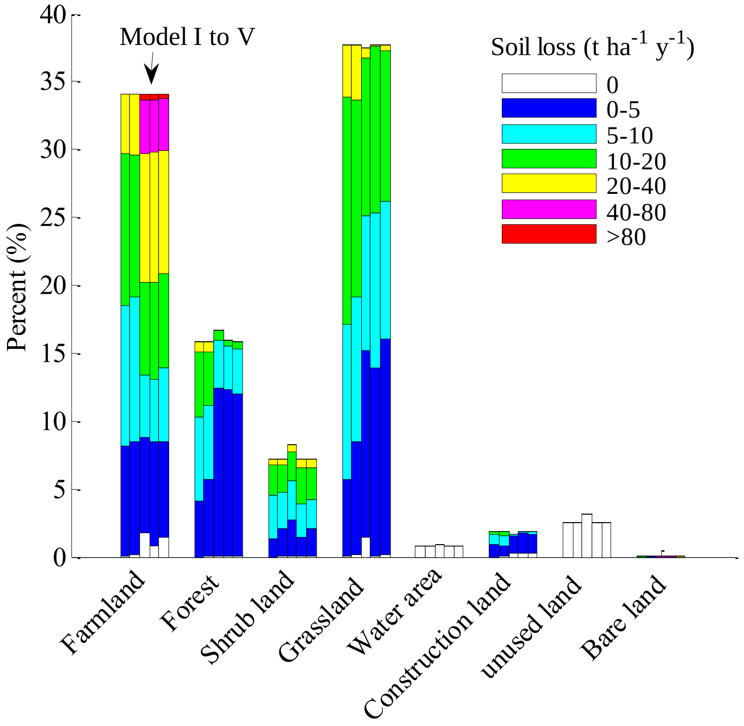

Figure 7: Proportion of soil erosion intensity levels for different land use for five models.

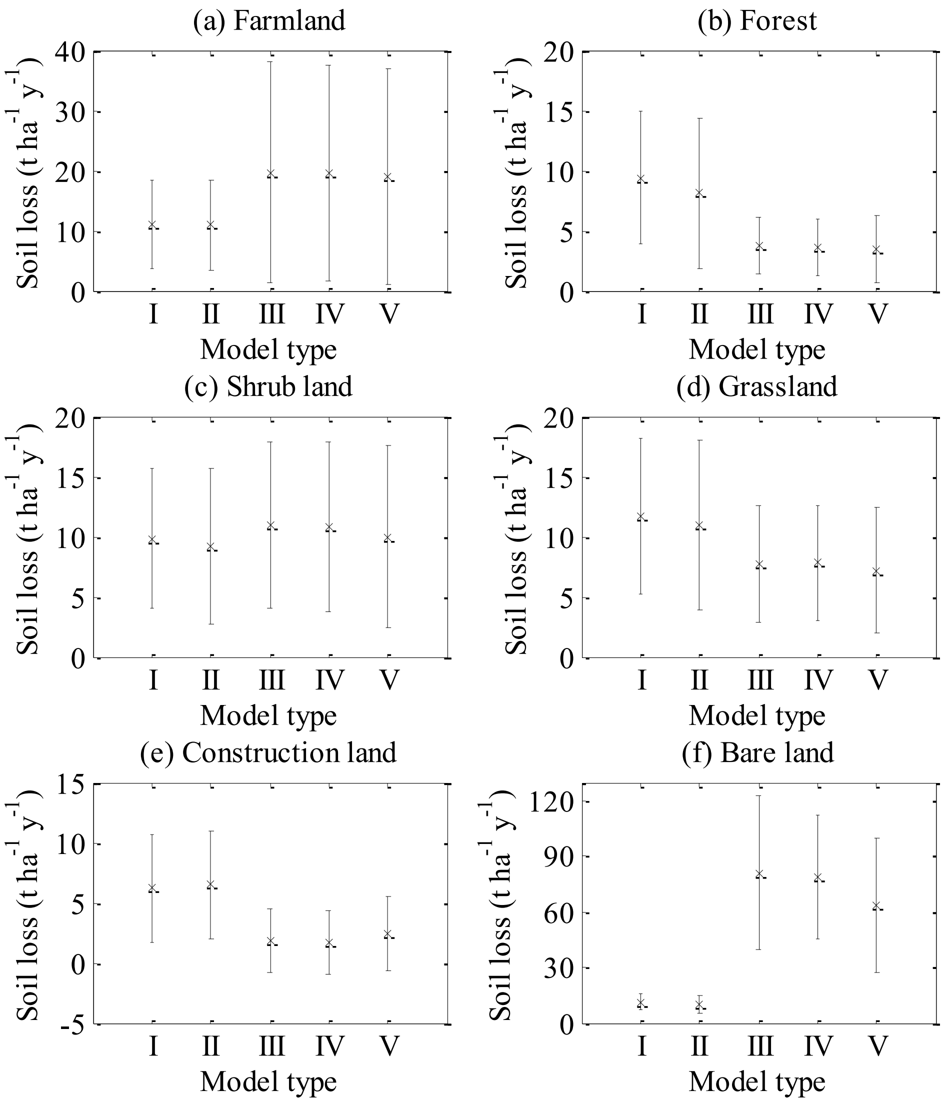

Figure 8: Error bar plot of soil loss rates for five models for different land uses: (a) Farmland; (b) Forest; (c) Shrub land; (d) Grassland; (e) Construction land; (f) Bare land. The star symbols stand for the mean values and the error bars stand for standard deviations.

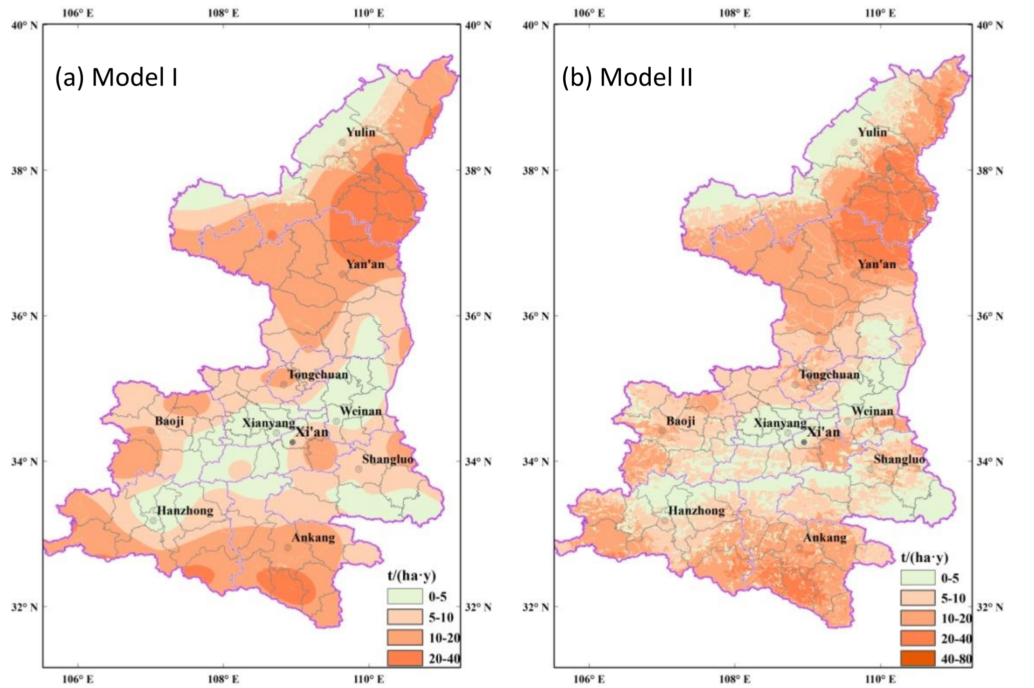
(a) Model I
(b) Model II
106° E
108° E
110° E
40° N
38° N
36° N
34° N
32° N
Yulin
Yan'an
Tongchuan
Baoji
Xianyang
Xi'an
Weinan
Shangluo
Hanzhong
Ankang
t/(ha·y)
0-5
5-10
10-20
20-40
40-80

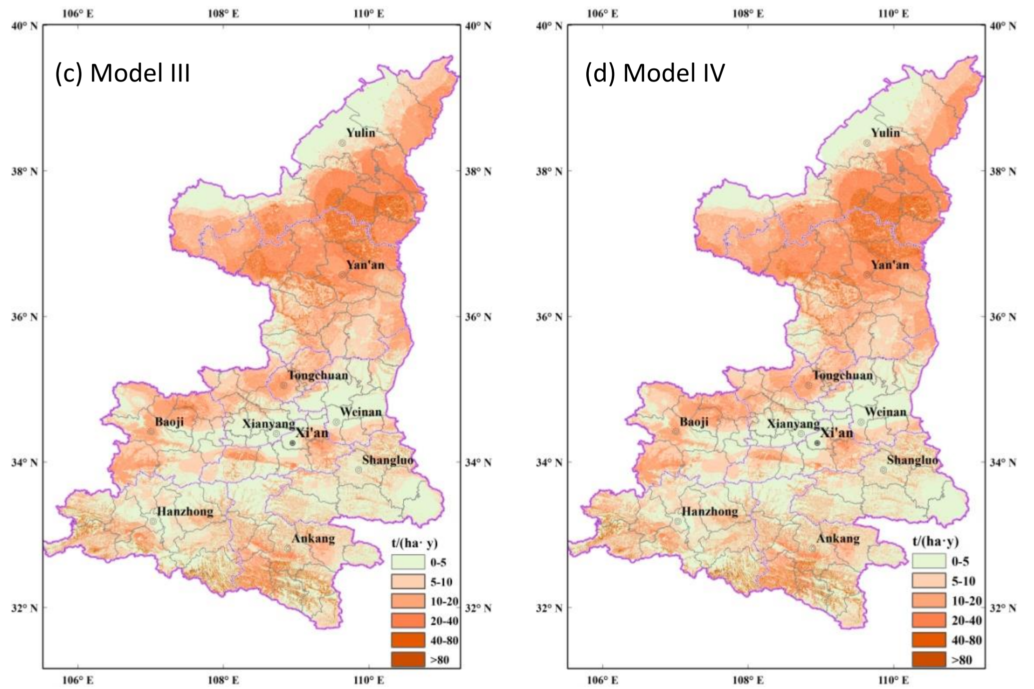
(c) Model III
(d) Model IV
106° E
108° E
110° E
40° N
38° N
36° N
34° N
32° N
Yulin
Yan'an
Tongchuan
Baoji
Xianyang
Xi'an
Weinan
Shangluo
Hanzhong
Ankang
t/(ha·y)
0-5
5-10
10-20
20-40
40-80
>80

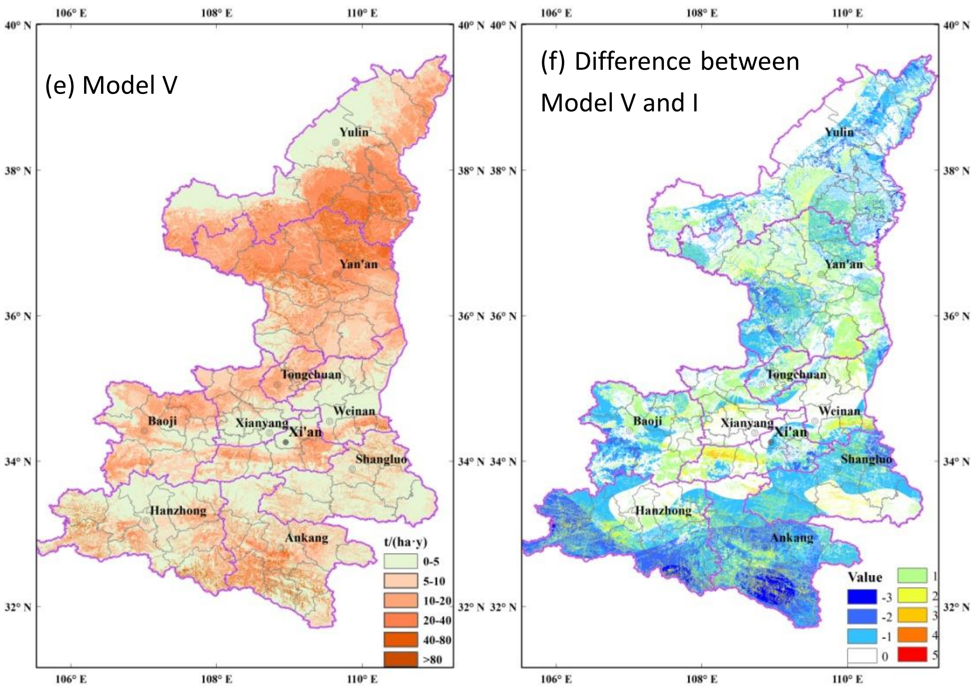

Figure 9: Distribution of soil erosion intensity levels for five models: (a) Model I; (b) Model II; (c) Model III; (d) Model IV; (e) Model V; (f) Difference between Model V and I. The levels of less than 5, 5-10, 10-20, 20-40, 40-80, greater than 80 t ha^{-1} y^{-1} were defined as the levels 1-6, respectively and the difference was the deviation of levels for Model V from Model I.